Experimental Thermal and Fluid Science 100 (2019) 319–327

Contents lists available at ScienceDirect

Experimental Thermal and Fluid Science

journal homepage: www.elsevier.com/locate/etfs

Gas flow rate measurement in low-quality multiphase flows using Venturi and gamma ray

Yanzhi Pan[a,b], Chao Li[c], Yugao Ma[c], Shanfang Huang[c], Dong Wang[a,*]

[a] State Key Laboratory of Multiphase Flow in Power Engineering, Xi'an Jiaotong University, Xi'an 710049, China
[b] Haimo Technologies Group Corp., Lanzhou 730050, China
[c] Department of Engineering Physics, Tsinghua University, Beijing 100084, China

ARTICLE INFO

Keywords:
Multiphase flow
Venturi meter
Gamma ray
Gas flow rate
Flow regime

ABSTRACT

Online flow rate measurements are encountered in many areas with a great need for high accuracy, especially in low-quality (0–0.1) flows. This paper concerns gas flow rate measurements using a Venturi meter and gamma-ray attenuation technique. A linear correlation is developed to predict the gas flow rates with wide ranges of void fractions (0–95%). The correlation predictions were compared to experimental data in which the root mean square errors of the oil-air-water multiphase flow prediction results are 7.72%, 8.93% and 9.11% for the gas flow rate, the quality and the gas-liquid slip ratio, respectively. The effect of the Venturi size was tested, and the metering accuracy is found to increase with the inlet diameter. The prediction accuracy is improved for three-phase flows than for the corresponding two-phase flows due to the oil-water stirring in the three-phase flows. The analyses of the results indicate that the measurement accuracy is higher with stable flow regimes than intermittent flow regimes. The present method can be widely applied to both two-phase and three-phase flows in the oil industry even for different Venturis and fluid media.

1. Introduction

Low-quality (0–0.1) multiphase flows are commonly encountered in the petroleum industry, particularly in crude oil extraction and processing. An important parameter in multiphase flows is the flow rate (by volume or mass) of each individual phase. The traditional method used in industry is to separate each phase and then to measure the single-phase flow rates separately. Differential-pressure devices, e.g. Venturi or orifice meters, are the most commonly used devices [1]. However, the separation method is expensive and needs large space. Online multiphase flow rate measurement is a good choice that eliminates the deficiencies of the separation method. Therefore, there is a need to develop an efficient online multiphase flow rate measurement method [2].

Normally, online multiphase flow rate measurements are based on conventional single-phase measurement methods, such as differential-pressure methods. Venturi meters are the most commonly used differential-pressure devices for multiphase flows [3]. The smooth flow profile in a Venturi meter reduces the frictional loss, which increases the reliability of the device and improves the pressure recovery [4]. A number of studies have been published to describe applications of Venturi meters in multiphase flows [5–10].

Gas flow rate is an important parameter and should be accurately measured to characterize the multiphase flows. Gas flow rate measurements by differential-pressure devices generally need another parameter, e.g. void fraction. Popular methods used to measure void fractions are based on electrical impedance technique or gamma-ray attenuation technique [11]. Electrical impedance technique has been widely used in laboratories, owing to its safety and low cost [12–14]. However, the relative permittivities or conductivities of the monitored phases cannot be assumed to remain constant during the whole life of an oil well. Changes in these parameters will result in measurement errors for the electrical impedance technique. By contrast, gamma attenuation technique is widely used in the commercial oil industries to measure the void fractions since it is non-intrusive, reliable, sensitive and robust [15,16].

Besides direct experimental metering facilities, calculation models are also necessary in online gas flow rate measurements. When a Venturi meter is used to measure multiphase flows, the basic assumptions are that all phases are homogeneous and travelling at the same velocity. However, these ideal conditions rarely exist in practice. Hence, a correction factor is required to compensate for the flow's deviation from non-slip condition. A large number of correlations have been developed for differential-pressure flowmeters regarding two-

* Corresponding author.
E-mail address: wangdong@mail.xjtu.edu.cn (D. Wang).

https://doi.org/10.1016/j.expthermflusci.2018.09.017
Received 6 March 2018; Received in revised form 9 August 2018; Accepted 25 September 2018
Available online 26 September 2018
0894-1777/

Table 1
Typical multiphase flow measurement studies.

Author	Year	Test fluid	Pressure (Bar)	Quality (%)	Metering technique
Murdock [17]	1962	Steam-water	39.6–40.3	78.0–95.0	Orifice
James [18]	1965	Steam-water	7.7–16.8	6.2–66.9	Orifice
Chisholm [19]	1974	Steam-water	10.0–70.0	0–15.0	Orifice
Lin [20]	1982	R113 Vapor-liquid	19.6–28.6	0–100.0	Orifice
Zhang [21]	1992	Air-water	2.0–3.2	0–1.0	Orifice + quick closing valve
Zhang et al. [22]	2005	Oil-water	2.0–4.0	0–2.0	Venturi meter + ECT
Huang et al. [23]	2005	Oil-gas	2.0–4.0	0–2.0	Venturi meter + ECT
Yuan et al. [24]	2015	Air-water	6.0–14.0	30.0–100.0	Venturi meter

Note: ECT refers to electrical capacitance tomography.

phase flows [17–29], such as Murdock correlation [17], Lin correlation [20], and Chisholm correlation [27,28]. These correlations are mostly nonlinear, whereas a linear correlation would more effectively improve the prediction accuracy.

Table 1 lists typical multiphase flow measurement studies [17–24]. It shows that most existing researches have focused on either multiphase flows under high pressure [17–20] or very low quality cases of 0–2% under low pressure [21–23], both of which do not cover the complete ranges of actual oilfield multiphase flows. In addition, these studies have been mainly intended for either two-phase flows or three-phase flows [30]. Hence, a general correlation is needed to cover both two-phase and three phase flows.

The objective of this work is to develop an online method for gas flow rate measurements in low-quality multiphase flows (0–0.1) under low pressure (1.5–6.0 bar). The void fraction of the flow has a wide range from 0% to 95%. A linear correlation was first developed based on the modified separated flow model from a linear regression. Then a Venturi and the gamma attenuation technique were experimentally used to precisely measure the pressure drop and void fraction, and further to predict gas flow rate. Finally, different factors including geometrical size and fluids properties were tested to see how they affect the measurement accuracies.

The organization of the paper is as follows. Section 2 deduces the linear correlation. Section 3 describes the experimental set up. Section 4 presents the experimental results and discusses the key effects. Finally, Section 5 summarizes the conclusions.

2. Theoretical description

The pressure difference from the inlet to the nozzle throat is measured through a Venturi meter. In single-phase gas flows, the relationship between the gas flow rate and the pressure difference is defined as:

$$\begin{aligned} Q_{g,1} &= \frac{\varepsilon C}{\sqrt{1-\beta^4}}\sqrt{2}A\sqrt{\frac{\Delta p}{\rho_g}} \\ W_{g,1} &= \frac{\varepsilon C}{\sqrt{1-\beta^4}}\sqrt{2}A\sqrt{\Delta p \rho_g} \end{aligned} \tag{1}$$

where $Q_{g,1}$ and $W_{g,1}$ are the gas volumetric and mass flow rates of the single-phase gas flow, ε is the expansion coefficient, C is the Venturi discharge coefficient, A is the Venturi throat area, ρ_g is the gas density, Δp is the pressure difference, and$\beta$is the throat ratio.

Different phases in multiphase flows are not travelling at the same velocity due to the slip between phases. Therefore, the original correlations used for the single-phase flow need to be modified when applied to multiphase flows. Several models have been developed for two-phase flows and the separated flow model is a popular one [20,31]. This model assumes thermodynamic equilibrium between the two phases. The gas and liquid phases are regarded as two continuous fluids without momentum exchange or phase change. According to the separated flow model, the gas flow rate of a two-phase flow is defined as:

$$\begin{aligned} Q_{g,2} &= \alpha Q_{g,1} \\ W_{g,2} &= \alpha W_{g,1} \end{aligned} \tag{2}$$

where $Q_{g,2}$ and $W_{g,2}$ are the gas volumetric and mass flow rates in multiphase flow defined by the separated flow model, α is the void fraction. When α equals 1, Eq. (2) simplifies to Eq. (1). However, Eq. (2) cannot accurately describe the real condition that contains both momentum exchange and phase change. Thus, a modified coefficient, ϕ, is introduced into Eq. (2).

$$\begin{aligned} Q_g &= \phi Q_{g,2} \\ W_g &= \phi W_{g,2} \end{aligned} \tag{3}$$

From Eq. (3), ϕ can be deduced as:

$$\phi = \frac{W_g}{\frac{\varepsilon C}{\sqrt{1-\beta^4}}\sqrt{2}A\alpha\sqrt{\frac{\Delta p}{\rho_g}}} \tag{4}$$

Similar to Eq. (1), the total flow rates of the gas-liquid two-phase flow can be defined by:

$$W_{tp} = \frac{\varepsilon C}{\sqrt{1-\beta^4}}\sqrt{2}A\sqrt{\Delta p(\rho_g \alpha + \rho_l(1-\alpha))} \tag{5}$$

where W_{tp} is the mass flow rate of the gas-liquid two-phase flow, ρ is the density, and the subscripts g and l refer to the gas and liquid single-phase flows, respectively.

From Eqs. (4) and (5), ϕ can also be defined as:

$$\phi = \frac{x}{\alpha}\sqrt{\alpha + (1-\alpha)\frac{\rho_l}{\rho_g}} \tag{6}$$

where $x = W_g/W_{tp}$ is the quality in the multiphase flow [32].

The gas-liquid slip ratio, S, is a function of the void fraction, α, and the gas quality, x.

$$S = \frac{\rho_l}{\rho_g}\left(\frac{1}{\alpha}-1\right)\left(\frac{x}{1-x}\right) \tag{7}$$

Assuming that the gas and liquid viscosities are constants, the gas-liquid slip ratio can be defined as a function of the density ratio, ρ_g/ρ_l [17,26]:

$$S = f\left(\frac{\rho_g}{\rho_l}\right) \tag{8}$$

Eqs. (6)–(8) can be combined to deduce ϕ as a single function of α. It should be noticed that α is not an independent variable, but rather it is a parameter related to the flow features such as the velocity, density ratio and gas-liquid slip ratio.

In this paper, the reference modified coefficient, ϕ, used to obtain the empirical correlations, will be determined from obtained data of various Δp, α and Q_g through Eq. (4). Fan et al. [33] developed a correlation with exponential form which showed good agreement with experiments. Similarly, by processing the data of various parameters, we figured out the linear relationship between $\ln(\alpha\phi)$ and α:

$$\ln(\alpha\phi) = a\cdot\alpha + b \tag{9}$$

where the constants a and b are the slope and the intercept determined

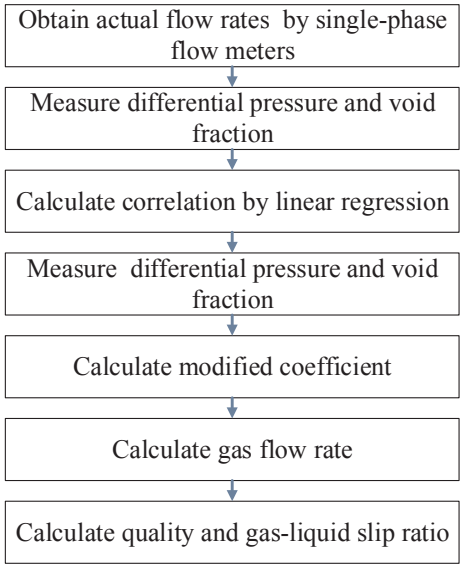

Fig. 1. Flowchart for determining the gas flow rate, quality and gas-liquid slip ratio.

from the experimental data.

The correlation can then be used to predict the modified coefficient, ϕ_c, and the gas flow rate, Q_g, after the void fraction and pressure drop have been obtained.

$$\phi_c = \frac{e^{a\alpha+b}}{\alpha} \tag{10}$$

$$Q_g = \phi_c Q_{g,2} \tag{11}$$

For typical gas-liquid-liquid three-phase flows in the oil industry, the gas, oil and water densities are around 1 kg/m^3, 875 kg/m^3 and 1000 kg/m^3, respectively. The gamma-ray absorption coefficient for the gas is negligible since the coefficient is as high as 0.13 cm^{-1} and 0.16 cm^{-1} for oil and water, respectively. Therefore, the gas phase can be easily distinguished in the mixture. Thus, for gas flow rate measurements, the oil and water mixtures are normally considered a single phase in an oil-gas-water three-phase flow.

The flowchart for measuring the gas flow rate, as well as the quality and the gas-liquid slip ratio, based on the modified separated flow model is shown in Fig. 1. First, the actual flow rate of each phase is obtained by single-phase flow meters, and the void fraction is measured by the gamma ray detector. Second, the empirical coefficients in Eq. (9) are determined from a linear regression of the data. The empirical correlations are then used to predict the modified coefficient. Then, the gas flow rate can be determined using Eq. (11). After the quality is calculated, the gas-liquid slip ratio can be obtained using Eq. (7).

3. Experimental apparatus and method

3.1. Flow loop

Fig. 2 shows a diagram of the multiphase flow loop with the fluids of transformer oil, air and tap water. The Venturi meter and gamma-ray densitometer were installed on the vertical test section. Single-phase oil, gas and water flows were first pumped into the single-phase flow meters before entering the mixer. The multiphase flow was then measured in the vertical test section. The two-phase or three-phase flow then entered the separator downstream of the test section to be separated and recycled.

The commercial single-phase flow meters have accuracies within 0.2% of the full scale readings. Hence, the measured single-phase flow rates were regarded as the reference data. The temperature and operating pressure sensors in the flow loop have an accuracy within 0.075% of the full scale reading. The experiments were performed at pressures between 1.5 and 6.0 bar with an operating temperature of 20 °C. Transformer oil, air and tap water were used as the test fluids and their densities at 20 °C are listed in Table 2. The density of air is much lower than that of oil or water.

Table 3 lists the experimental conditions including the gas and total liquid (oil plus water) flow rates. The flows were measured for void fractions between 0 and 95% with wide ranges of the test fluid flow rates. Two kinds of pipe diameter, DN50 and DN80, were used in the experiments.

3.2. Test section

Fig. 3 shows a schematic of the Venturi meter installed vertically in the test section. The multiphase flow was first pumped into the inlet at the bottom, and then went upward through the Venturi tube. The differential pressure and the operating pressure were measured by high-precision sensors made by the ROSEMOUNT Company with an accuracy 0.075% of the full scale reading.

As shown in Fig. 3, a gamma-ray densitometer was installed at the Venturi throat to measure the void fraction. The gamma-ray densitometer included a gamma source and a detector. The intensity decayed as the gamma rays passed through the multiphase flow in the pipeline. The cone beam did not cover the entire cross section of the channel but only a wedge-shaped segment. The experiments used the encapsulated 50 mCi Am-241 gamma sources for the DN50 Venturi meters and the encapsulated 100 mCi Am-241 gamma sources for the DN80 Venturi meters.

The gamma rays are collimated before passing through the mixture and accepted after a 2-cm diameter hole. The void fraction was determined by measuring the average effective linear attenuation coefficient in the measurement volume over the pipe cross-section [34]. Since the test section was installed in a vertical pipeline, the line void fraction was assumed to be independent of the measurement angle. The void fraction was then calculated by:

$$\alpha = \frac{\ln(I/I_l)}{\ln(I_g/I_l)} \tag{12}$$

where I, the transmitted intensity, is a function of the fractions of gas and liquid in the flow. I_l and I_g are the calibrated intensities for pure liquid and gas, respectively. The sampling time was 15–30 min for each case and the void fractions were the time-averaged results of the readings.

Table 4 lists five kinds of test sections in the experiments. Two Venturi inlet diameters, 80 mm and 50 mm, were used with the throat ratios, β, of 0.45, 0.50, and 0.55. The Venturi meters and fluid media were combined to form nine sets of experimental data. Regarding the notation, DN80 (0.45) O-A-W means an oil-air-water three-phase flow measurement with a 80 mm inlet diameter and a 0.45 throat ratio for Venturi.

4. Results and discussion

This section presents the typical metering results for DN50 (0.50) O-A-W condition, including the modified coefficient, ϕ, the gas flow rate, the mass quality, the gas-liquid slip ratio, and their corresponding errors. The effects of Venturi size and the fluid properties are then analyzed by comparing the metering results for the different experimental series.

4.1. Typical results

4.1.1. Modified coefficient, ϕ

The results for experimental case DN50 (0.50) O-A-W are shown in

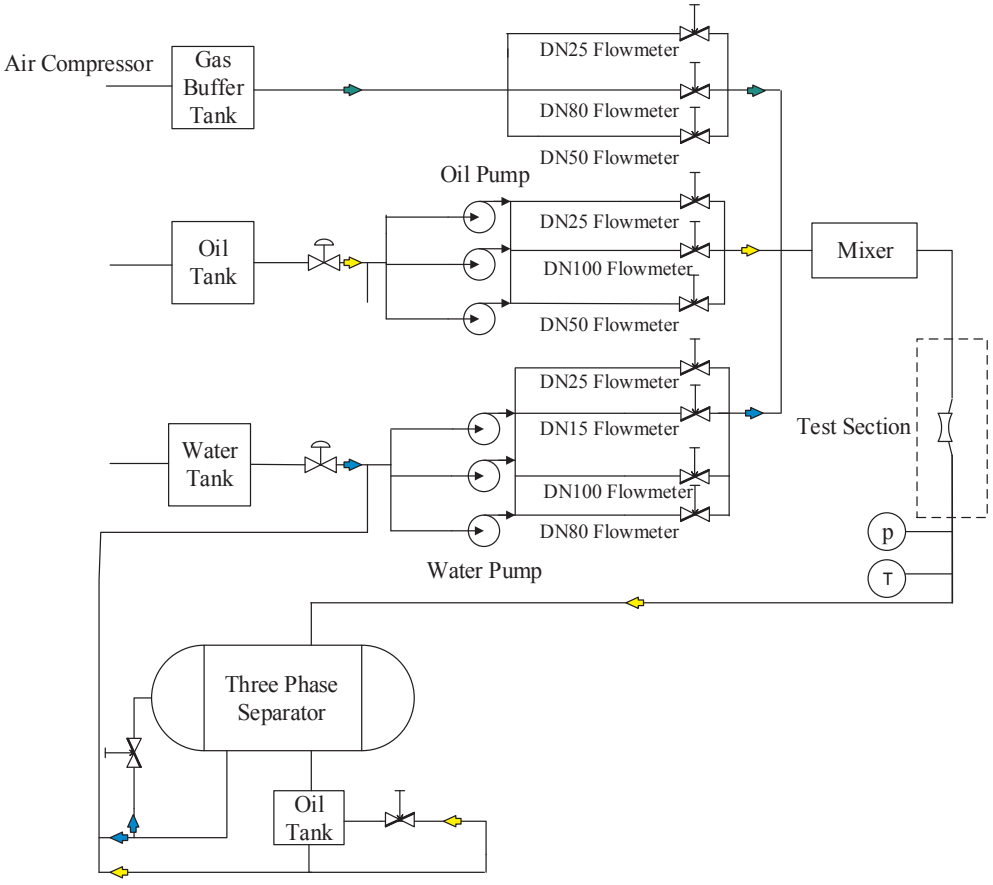

Fig. 2. Schematic diagram of the flow loop.

Table 2
Experimental conditions and measurement uncertainties.

Conditions	Range	Uncertainty
Temperature	20 °C	0.075%
Densities	1.204 kg/m^3 (air, 20 °C) 998.5 kg/m^3 (water, 20 °C) 875.2 kg/m^3 (transformer oil, 20 °C)	0.5%
Pressure	1.5–6.0 bar	0.075%

Table 3
Experimental conditions.

Experimental ranges	DN80	DN50
Total liquid flow rate (m^3/h)	7.0–74.0 (0.39–4.10 m/s)	4.5–27.0 (0.64–3.80 m/s)
Gas Flow rate (m^3/h)	7.0–380.0 (0.39–21.00 m/s)	4.6–82.0 (0.65–11.60 m/s)
Water cut	0–100%	0–100%
Void fraction	0–95%	0–90%

Note: DN means the nominal pipe diameter, and the water cut refers to the mass fraction of water in the oil-water mixture.

Figs. 4–8. Fig. 4 presents the linear regression results between the reference modified coefficient, ϕ_r from Eq. (4), and the void fraction, α. The correlation for the modified coefficient for DN50 (0.50) O-A-W condition is:

$$\ln(\alpha\phi_c) = 4.474\alpha - 5.324 \quad (13)$$

where ϕ_c is the calculated modified coefficient. As shown in Fig. 4, the results have good linearity.

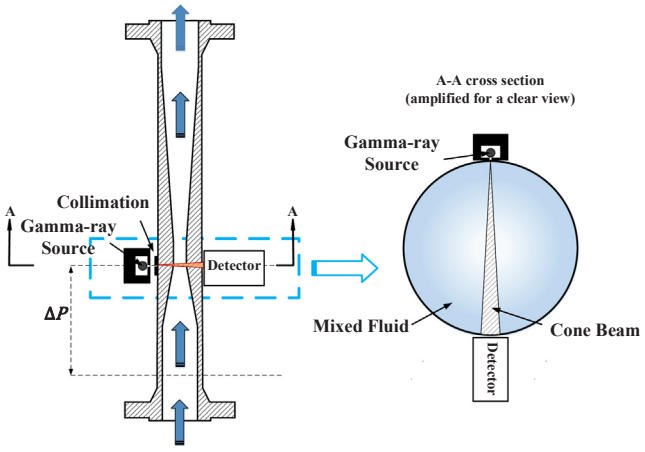

Fig. 3. Schematic of the test section.

Table 4
Venturi meter sizes used in the experiments.

Inlet diameter (mm)	Throat ratio	$\frac{\sqrt{2}\varepsilon CA}{\sqrt{1-\beta^4}}$
DN80	0.45	4.862
	0.55	7.502
DN50	0.45	2.0556
	0.5	2.163
	0.55	3.1409

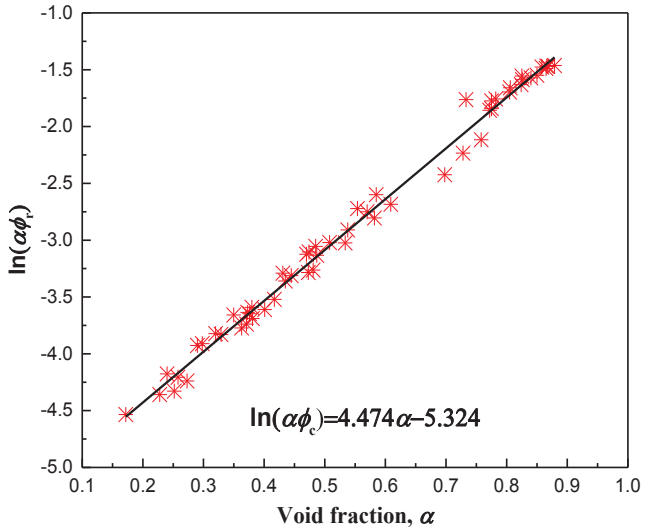

Fig. 4. Linear regression between ϕ_r and α for DN50 (0.50) O-A-W condition.

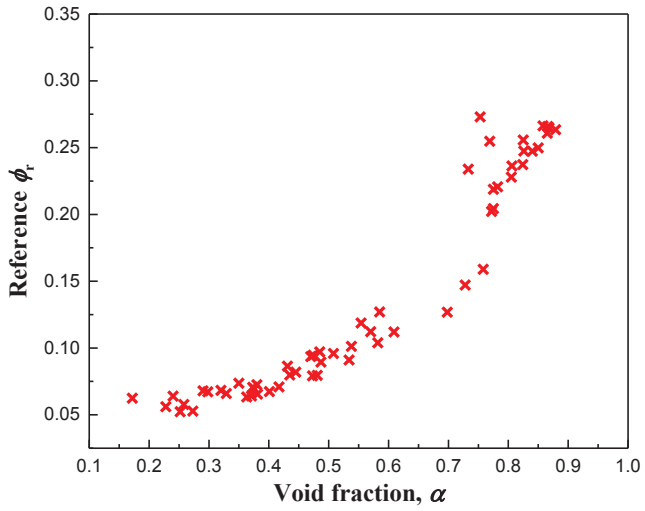

Fig. 5. Relationship between ϕ_r and α for DN50 (0.50) O-A-W condition.

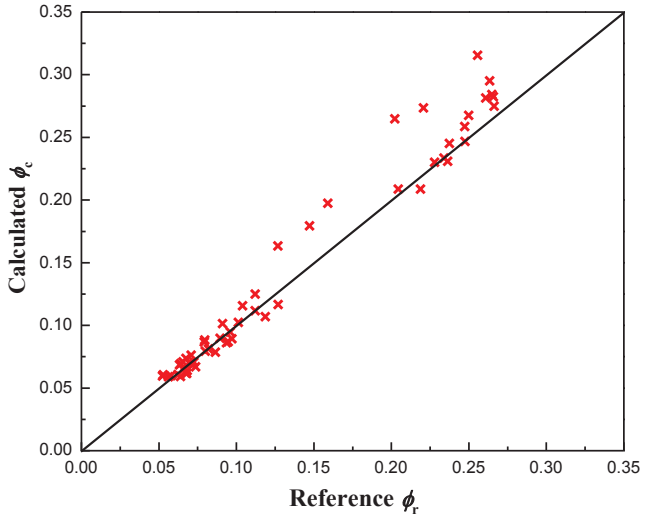

Fig. 7. Comparison of the reference ϕ_r and the calculated ϕ_c for DN50 (0.50) O-A-W condition.

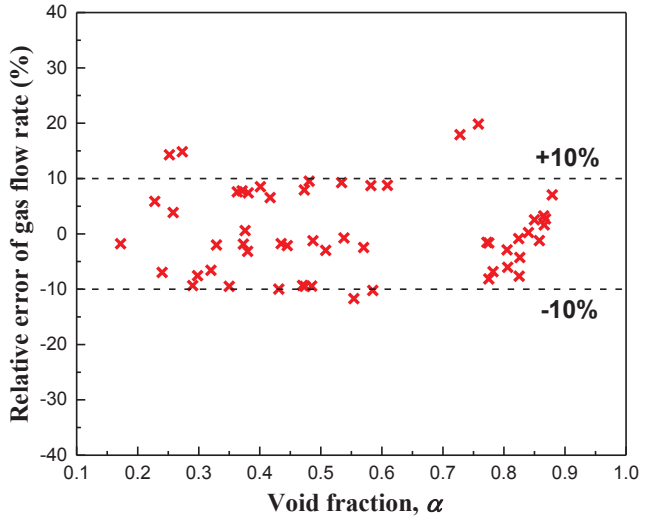

Fig. 8. Relative error between the calculated and reference gas flow rates for DN50 (0.50) O-A-W condition.

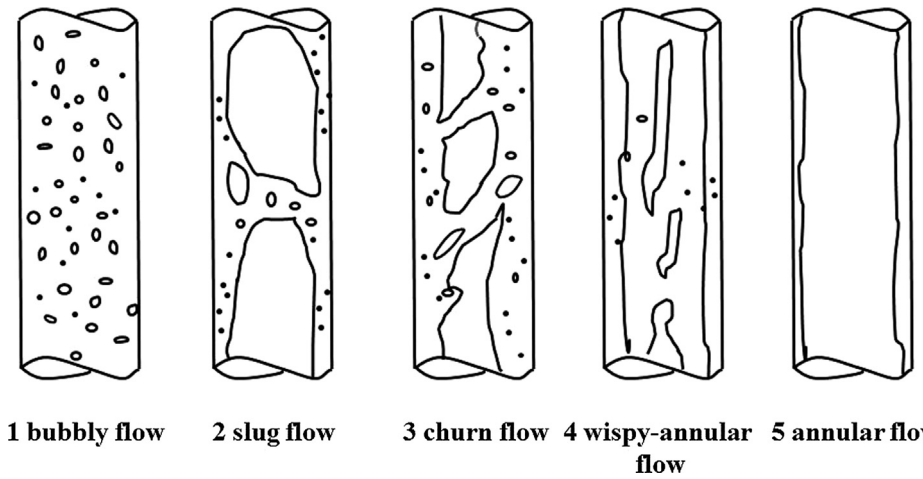

Fig. 6. Flow regimes in vertical pipes [34].

ϕ_c can then be determined from Eq. (13) once α is known. Thus, Eq. (13) can be used to estimate the multiphase flow parameters in practical applications.

Fig. 5 shows the relationship between ϕ_r and α to analyze the effect of the flow regimes on ϕ_r. The relationship between the reference coefficient and the void fraction is not linear due to the friction pressure drop. Generally, multiphase flow friction losses increase with the void fraction. Meanwhile, the pressure drop, Δp, is proportional to $1/\phi^2$ from Eq. (3). Thus, when the frictional pressure drop increases with void fraction, ϕ_r is relatively weakened. The deviation of the experimental data forming the comprehensive trend, α = 0.7–0.75, is due to the intermittent flow pattern.

Fig. 6 shows diagrams of typical flow regimes in vertical pipes which are defined as bubbly flow, slug flow, churn flow, wispy-annular flow and annular flow. The flow regime transitions are arranged in terms of increasing α.

Among the five flow regimes, the bubbly flow and annular flow regimes are stable. By contrast, the slug and churn flows are intermittent flows, which significantly affect the metering accuracy. The separated flow model assumes that the velocity of each phase is constant. However, the buoyancy has a significant effect on intermittent flows which results in different velocities of gas and liquid phases. This is one source of the measurement errors during intermittent flows. Another error source is the random measurement differences. Intermittent flows are instable flow patterns characterized by oscillating flowrates and pressures. Due to the limited sampling time, the measured results of intermittent flows will have higher uncertainty that also leads to the dispersion of the results in Fig. 5.

Fig. 7 compares the calculated coefficient, ϕ_c, and the reference coefficient, ϕ_r. For $\phi_r > 0.125$, the void fractions are greater than 0.6 in Fig. 5 that indicate the intermittent flow pattern. In Fig. 7, when ϕ_r is less than 0.125, the calculated coefficients agree well with the reference coefficients. When ϕ_r is larger than 0.125, ϕ_c gradually deviates from ϕ_r due to intermittent flow pattern.

After calculating the modified coefficient, the gas flow rates for DN50 (0.50) O-A-W condition can be calculated from Eq. (11). Fig. 8 illustrates the relationship between the void fraction and the relative error to describe the flow pattern impact on calculation accuracy. The relative error of gas flow rate (Fig. 8) is defined as $\varepsilon = \frac{Q_{\text{predicted}}(\alpha) - Q_{\text{reference}}(\alpha)}{Q_{\text{reference}}(\alpha)} \times 100\%$, where $Q_{\text{reference}}(\alpha)$ is determined by inlet single-phase flow meters and regarded as the reference, and $Q_{\text{pridicted}}(\alpha)$ is calculated by the model in this work.

During the intermittent flow (α at 0.7–0.75), relative differences are relatively high. For $\alpha > 0.77$, the flow regime gradually transforms to annular flow that again satisfies the requirement for the separated flow model and the relative differences decrease to less than 10%. The average overall difference is relatively low with a root mean square error (RMSE) of 7.72%. Thus, the measurement and calculation methods are reasonable and have high accuracy, especially for annular flow.

4.1.2. Gas-liquid slip ratio and quality

The gas-liquid slip ratio and the quality were also calculated based on the modified separated flow model. This section presents typical results for those two parameters for DN50 (0.5) O-A-W condition.

The gas-liquid slip ratio and the quality deduced from Eqs. (5) and (6) are:

$$x_c = \frac{\phi_c \alpha}{\sqrt{\alpha + (1-\alpha)\frac{\rho_L}{\rho_g}}} \tag{14}$$

$$S_c = \left(\frac{1}{\alpha} - 1\right)\left(\frac{x_c}{1-x_c}\right)\frac{\rho_L}{\rho_g} \tag{15}$$

where x_c is the calculated quality and S_c is the calculated gas-liquid slip ratio.

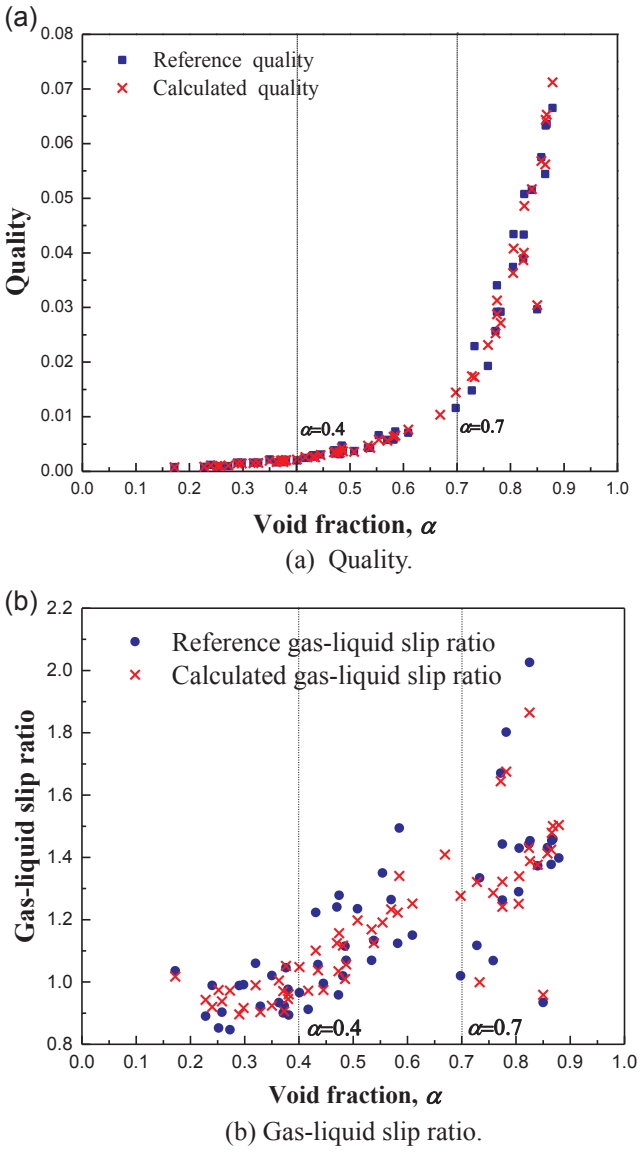

Fig. 9. Calculated characteristic parameters for the multiphase flow.

Fig. 9 presents the calculated results for those two parameters to characterize the multiphase flow with comparisons to the reference values. The calculated results are consistent with the reference data. The results can be divided into three parts according to the void fraction range.

For void fractions less than 0.4, the flow regime is bubbly flow in which the dispersed gas is entrained into the continuous liquid as small bubbles. Considering the large density difference between the gas and the liquid, the gas mass fraction is negligible and the gas-liquid slip ratios do not exceed 1.

For void fractions between 0.4 and 0.7, the bubbles become lager and the flow pattern transforms first into plug flow and then slug flow. The quality also increases and the buoyancy effect cannot be neglected anymore. The buoyancy causes the gas phase to flow faster than the liquid phase, so the slip ratio increases to greater than 1. The reference values are more dispersed than the calculated results, indicating that the approximate processing of the modified separated flow model weakens the real dispersion of slip ratios.

For void fractions larger than 0.7, the flow regime changes to slug flow, churn flow and annular flow as the quality increases rapidly and most of the flow channel is occupied by gas. Since churn flow is

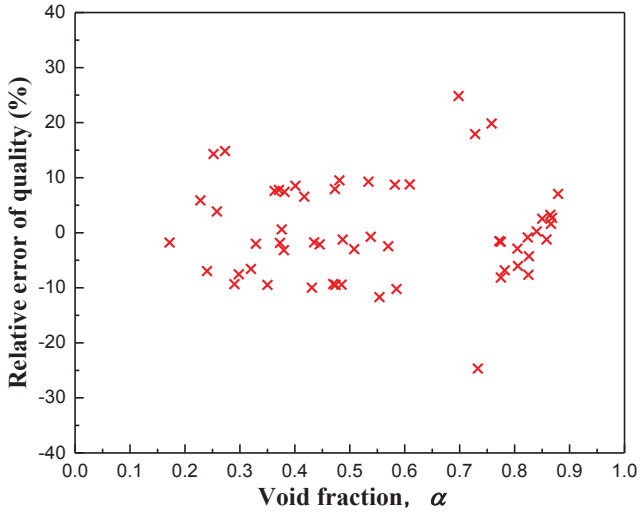

Fig. 10. Relative error in the quality for DN50 (0.50) O-A-W condition.

characterized by large waves travelling along the liquid film, the metering slip ratios vary between 0.9 and 2.1.

Fig. 10 shows the relative errors in the calculated quality for the DN50 (0.50) O-A-W case. Since x_c is determined from ϕ_c, the calculated errors in x_c depend on those in ϕ_c. Thus, the results in Fig. 10 have very similar trends to those in Fig. 8. For $0.7 < \alpha < 0.75$, the errors are relatively large while for $\alpha > 0.77$ the errors decrease significantly. The error trends also show that the flow pattern can be estimated to be intermittent flow for $0.7 < \alpha < 0.75$ and annular flow for $\alpha > 0.77$. The standard deviation of the calculated quality is 8.93%.

Fig. 11 shows the relationship between the void fraction and the gas volume fraction. It results from the changes of slip ratios. For slip ratios less than 1, the gas velocities are lower than the liquid velocities and the void fractions are larger than the gas volume fractions. As α increases, S gradually increases to greater than 1 and then the gas volume fractions begin to exceed the void fractions.

Similarly, since S_c is determined from x_c, the errors in S_c also depend on ϕ_c. Despite the effects of the unstable flow patterns, the calculated gas-liquid slip ratios are in good agreement with the reference values with a standard deviation of 9.11%.

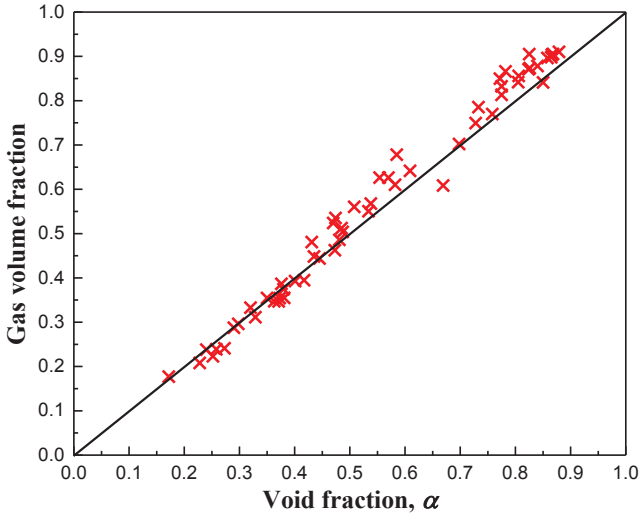

Fig. 11. Relationship between void fraction and the gas volume fraction for DN50 (0.50) O-A-W condition.

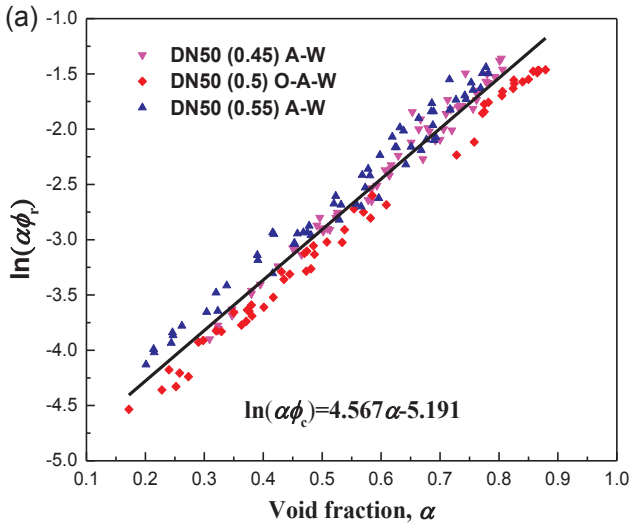

(a) DN50 Venturi meters.

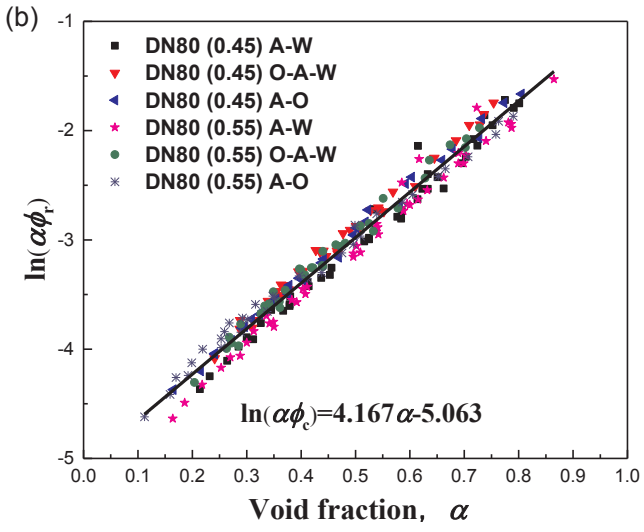

(b) DN80 Venturi meters.

Fig. 12. Linear regressions between $\ln(\alpha\phi_r)$ and α for two Venturi inlet diameters and various throat ratios.

4.2. Effects of Venturi meter size and fluid properties

Venturi meters with diameters of 50 mm (DN50) and 80 mm (DN80), were used to study the effects of Venturi size on the metering accuracy. The effects of the fluid properties were also studied.

Despite the gently varying cross section, the Venturi channel still modifies the flow pattern, which affects the metering accuracy. Fig. 12 shows the linear regression results of $\ln(\alpha\phi_r)$ as a function of α for all nine experimental series. Fig. 12(a) shows the data for DN50 test sections while Fig. 12(b) shows the data for DN80 test sections. The results show less dispersion of the data for the larger DN80 Venturi meters.

The data for the DN50 Venturi meters in Fig. 12(a) can be correlated as:

$$\ln(\alpha\phi_c) = 4.567\alpha - 5.191 \quad (16)$$

Similarly, the correlation of the data for the DN80 Venturi meters in Fig. 12(b) is

$$\ln(\alpha\phi_c) = 4.167\alpha - 5.063 \quad (17)$$

Then, Eqs. (16) and (17) are used to predict the gas flow rates of the multiphase flows measured by the DN50 and DN80 Venturi meters.

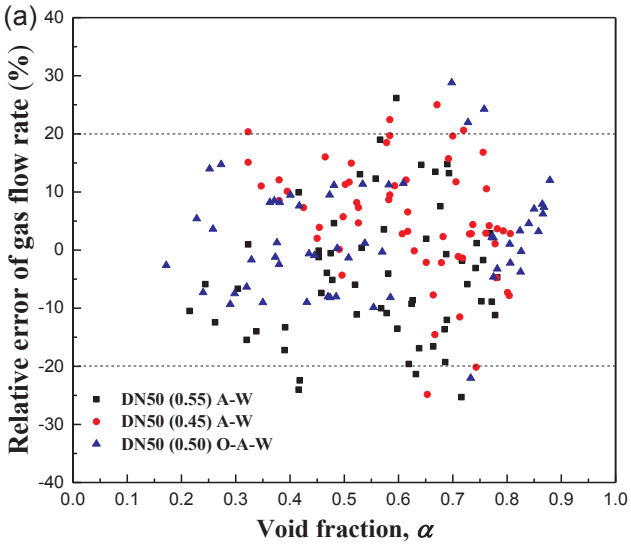

(a) Relative error in the gas flow rate measured by DN50.

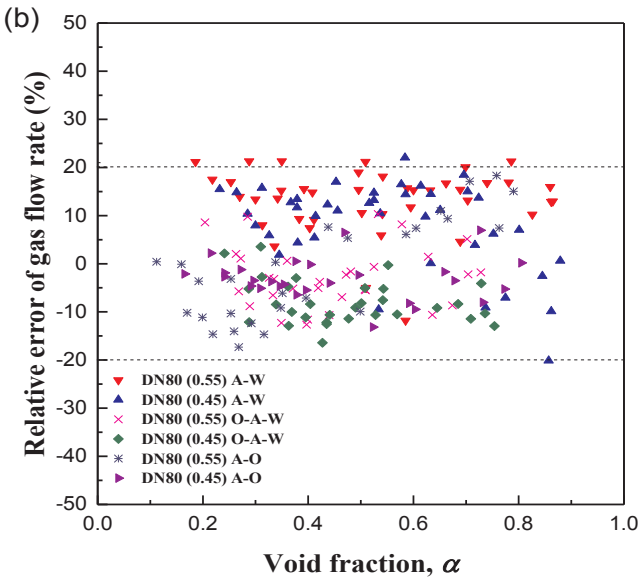

(b) Relative error in the gas flow rate measured by DN80.

Fig. 13. Influence of Venturi size on the metering accuracy.

Next, the predicted results are compared with the reference data to analyze the prediction accuracy. Fig. 13(a) shows that the relative errors in the DN50 data are larger than those in the DN80 data in Fig. 13(b). For example, the ± 20% error bands contain 86% of the relative deviations for DN50 while the ± 20% error bands contain 97% of relative deviations for DN80. Thus, the larger inlet diameter Venturi meters have the higher metering accuracies.

The separated flow model assumes that the gas-liquid slip ratio remains constant during the pressure drop measurement. However, the fluid accelerates while passing through the Venturi with different phase accelerating rates. Therefore, the void fraction at the Venturi throat differs from that at the inlet. This means that the flow pattern may change from the inlet to the throat. For example, slug flow at the inlet may become churn flow at the throat.

However, the void fractions in Eq. (4) are assumed constant from the upstream to the throat. These flow pattern transitions will affect the linear relationship between $\ln(\alpha\phi_r)$ and α deduced from Eq. (4). A Venturi with a small inlet diameter has more effect on the flow pattern stability due to the flow deformation, so larger diameter Venturi meters will tend to be more accurate. Even so, the metering accuracy of the DN50 Venturi is still acceptable with a root mean square error (RMSE) of 11%.

Table 5
Correlations for ϕ for the nine experimental series.

Venturi meter sizes		A-W	A-O	O-A-W
DN80	0.45	4.380α-5.243	4.269α-5.066	4.323α-5.047
	0.55	4.351α-5.252	3.870α-4.915	4.273α-5.070
DN50	0.45	4.859α-5.343	–	–
	0.5	–	–	4.474α-5.324
	0.55	4.431α-4.981	–	–

Table 6
RMSEs of the calculated gas flow rates for all nine experimental series.

Inlet diameter	β	A-W (%)	A-O (%)	O-A-W (%)
DN80	0.45	13.3	4.3	4.0
	0.55	9.2	9.9	5.1
DN50	0.45	10.1		
	0.5			7.9
	0.55	11.3		

Table 5 lists the linear regression correlations for all the nine experimental series including two Venturi inlet diameters, various throat ratios and three fluid combinations. The correlation coefficients are weakly dependent on the Venturi throat ratios and the test fluid with the coefficient a varying from 3.870 to 4.859 and the constant b varying from −5.343 to −4.915. Thus, the present correlation model is effective for both two-phase and three-phase flows measured by different Venturis.

Table 6 shows the root mean square errors (RMSEs) of calculated gas flow rates for the nine experimental series. The results show that:

(1) The measurement accuracies of three-phase flows are higher than those of the corresponding two-phase flows. For example, for the same Venturi size, DN80 (0.45), the gas flow rate root mean square errors (RMSEs) are 4.01% for the oil-air-water mixtures, 13.35% for the air-water mixtures and 4.25% for the oil-air mixtures. The high viscosity of the oil phase effectively mixes the fluid, which reduces the bubble sizes in the mixture. The flow patterns tend to be more homogeneous.
(2) The larger inlet diameter Venturi results in a higher accuracy. The errors listed in Table 6 show that the gas flow rates measured by the DN80 Venturi meters are generally more accurate than those measured by the DN50 Venturi meters since the flow patterns are more stable in the larger Venturi meter with weaker deformations.
(3) The average error is 8.66%, which is sufficient for practical applications.

5. Conclusions

An online method was developed to more accurately measure gas flow rates in low-quality (0–0.1) two-phase and three-phase flows. A liner correlation was presented to modify the calculation model. Various factors, e.g. Venturi size and the fluid properties, were tested to see how they affect the measurement accuracy. The following conclusions can be made.

(1) Single-energy gamma attenuation technique was used to measure the void fraction and a Venturi was used to measure the pressure drop. The present method can be widely applied to predict gas flow rates online in both two-phase and three-phase flows.
(2) A linear correlation was developed based on the modified separated flow model and experimental data to predict gas flow rates in multiphase flows. The void fraction of the flow has a wide range

from 0% to 95%. The linearity of the correlation effectively improves the prediction accuracy. The constants in the correlations, the coefficient a and constant b, are less affected by the Venturi throat ratios and the fluid properties. This means the present model has a good applicability to be used for different Venturis and fluid media.

(3) The present method has high measurement accuracy. The root mean square errors for DN50 (0.5) O-A-W condition are 7.72% for the gas flow rates, 8.93% for the quality and 9.11% for the gas-liquid slip ratio. The overall average root mean square error for all of the measured gas flow rates was 8.66%.

(4) Both the Venturi size and the fluid properties have weak effects on the measurement accuracy. The measurement accuracy is found to be higher in stable flow regimes than that in intermittent flow regime. Large inlet diameters result in high accurate results. The flow regimes for three-phase flows are more stable than the corresponding two-phase flows, leading to higher measurement accuracies for three-phase flows.

Conflict of interest

The authors declared that they have no conflicts of interest to this work.

We declare that we do not have any commercial or associative interest that represents a conflict of interest in connection with the work submitted.

Acknowledgements

The authors gratefully acknowledge the financial support provided by the National Science and Technology Major Project of China (Grant: 2016ZX05028-003-004).

References

[1] S.F. Huang, T.Y. Ma, D. Wang, Z.H. Lin, Study on discharge coefficient of perforated orifices as a new kind of flowmeter, Exp. Therm. Fluid Sci. 46 (2013) 74–83.
[2] G. Falcone, G.F. Hewitt, C. Alimonti, B. Harrison, Multiphase flow metering: current trends and future developments, J. Petrol. Technol. 54 (2002) 77–84.
[3] Y.Z. Pan, Y.G. Ma, S.F. Huang, P.M. Niu, D. Wang, J.H. Xie, A new model for volume fraction measurements of horizontal high-pressure wet gas flow using gamma-based techniques, Exp. Therm. Fluid Sci. 96 (2018) 311–320.
[4] H.A. Abbas, M. Hasan, G.P. Lucas, Experimental and theoretical study of the gas–water two-phase flow through a conductance multiphase Ventui meter in vertical annular (wet gas) flow, Nuc. Eng. Des. 241 (2011) 1998–2005.
[5] A.B. Olsen, B.V. Hanssen, Framo multiphase flowmeter-field testing experience from Statoil Gullfaks A and B platforms and Texaco Humble test facilities, in: 12th North Sea Flow Measurement Workshop, Peebles, Scotland, 1994, October 24–27.
[6] E.A. Hammer, J.E. Nordtvedt, The application of a Venturi meter to multiphase flow meters for oil well production, in: 5th Conference on Sensors and Applications, London, UK, 1991, September 22–25 (Bristol: Adam Hilger).
[7] A.B. Olsen, Framo subsea multiphase flow meter system, in: Multiphase Meters and their Subsea Applications Seminar, London, England, 1993.
[8] R.N. Steven, Wet gas metering with a horizontally mounted venturi meter, Flow Meas. Instrum. 12 (2002) 361–372.
[9] K. Olsvik, M. Marshall, T. Whitaker, Fluenta multiphase flow meter, tested and marinised, in: 13th North Sea Flow Measurement Workshop, Lillehammer, Norway, 1995, October 22–26.
[10] M.O. Elobeid, L.M. Alhems, A. Al-Sarkhi, A. Ahmad, S.M. Shaahid, M. Basha, J.J. Xiao, R. Lastrab, C.E. Ejim, Effect of inclination and water cut on Venturi pressure drop measurements for oil-water flow experiments, J. Petrol. Sci. Eng. 147 (2016) 636–646.
[11] R. Thorn, G.A. Johansen, B.T. Hjertaker, Three-phase flow measurement in the petroleum industry, Meas. Sci. Technol. 24 (2013) 012003.1-17.
[12] S.F. Huang, X.G. Zhang, D. Wang, Z.H. Lin, Water holdup measurement in kerosene–water two-phase flows, Meas. Sci. Technol. 18 (2007) 3784–3794.
[13] S.F. Huang, B. Zhang, J. Lu, D. Wang, Study on flow pattern maps in hilly-terrain air–water–oil three-phase flows, Exp. Therm. Fluid Sci. 47 (2013) 158–171.
[14] S.F. Huang, X.X. Wu, B.Y. Zong, et al., Local void fractions and bubble velocity in vertical air-water two-phase flows measured by needle-contact capacitance probe, Sci. Technol. Nucl. Install. 2018 (4) (2018) 1–14.
[15] S. Blaney, H. Yeung, Investigation of the exploitation of a fast-sampling single gamma densitometer and pattern recognition to resolve the superficial phase velocities and liquid phase water cut of vertically upward multiphase flows, Flow Meas. Instrum. 19 (2008) 57–66.
[16] C. Wang, N. Zhao, L. Fang, et al., Void fraction measurement using NIR technology for horizontal wet-gas annular flow, Exp. Therm. Fluid Sci. 76 (2016) 98–108.
[17] J.W. Murdock, Two-phase flow measurements with orifices, J. Basic Eng. 84 (1962) 419–433.
[18] R. James, Metering of steam-water two-phase flow by sharp-edged orifices, Proc. Inst. Mech. Eng. 180 (1965) 549–566.
[19] D. Chisholm, Pressure drop during steam/water flows through orifices, J. Mech. Eng. Sci. 16 (1974) 353–355.
[20] Z.H. Lin, Two-phase flow measurements with sharp-edged orifices, Int. J. Multiphase. Flow 8 (1982) 683–693.
[21] H.J. Zhang, S.J. Lu, G.Z. Yu, An investigation of two-phase flow measurement with orifices for low-quality mixtures, Int. J. Multiphase Flow 18 (1992) 149–155.
[22] H.J. Zhang, W.T. Yue, Z.Y. Huang, Investigation of oil–air two-phase mass flow rate measurement using venturi and void fraction sensor, J. Zhejiang Univ. Sci. 6A (6) (2005) 601–606.
[23] Z.Y. Huang, D.L. Xie, H.J. Zhang, H.Q. Li, Gas-oil two-phase flow measurement using an electrical capacitance tomography system and a venturi meter, Flow Meas. Instrum. 16 (2005) 177–182.
[24] C. Yuan, Y. Xu, T. Zhang, J. Li, H. Wang, Experimental investigation of wet gas over reading in Venturi, Exp. Therm. Fluid Sci. 66 (2015) 63–71.
[25] R. Steven, A dimensional analysis of two phase flow through a horizontally installed Venturi flow meter, Flow Meas. Instrum. 19 (2008) 342–349.
[26] R.V. Smith, J.T. Leang, Evaluations of correlations for two-phase flowmeters three current-one new, J. Eng. Power 97 (1975) 589–594.
[27] D. Chisholm, Flow of incompressible two-phase mixtures through sharped edged orifices, J. Mech. Eng. Sci. 9 (1967) 72–78.
[28] D. Chisholm, Research note: two-phase flow through sharp-edged orifices, J. Mech. Eng. Sci. 19 (1977) 128–130.
[29] R. De Leeuw, Liquid correction of Venturi meter readings in wet gas flow, in: North Sea Flow Measurement Workshop, Kristiansand, Norway, 1997, October.
[30] L.Y. Meng, Y.X. Li, J. Zhang, S.P. Dong, The development of a multiphase flow meter without separation based on sloped open channel dynamics, Flow Meas. Instrum. 22 (2011) 120–125.
[31] R. Lockhart, R. Martinelli, Proposed correlation of data for isothermal two-phase, two-component flow in pipes, Chem. Eng. Prog 45 (1949) 39–48.
[32] M. Woldesemayata, A. Ghajar, Comparison of void fraction correlations for different flow patterns in horizontal and upward inclined pipes, Int. J. Multiphase Flow 33 (2007) 347–370.
[33] G. Fan, C. Yan, X. Chao, et al., The experiment research on void fraction insteady vertical tubes, in: Chinese Society of Engineering Thermophysics Conference on Multiphase flow, 2006, (In Chinese).
[34] E. Åbro, G.A. Johansen, Improved void fraction determination by means of multi-beam gamma-ray attenuation measurements, Flow Meas. Instrum. 10 (1999) 99–108.